GEORGIA INSTITUTE OF TECHNOLOGY
OFFICE OF CONTRACT ADMINISTRATION
SPONSORED PROJECT INITIATION

Date: 12/10/80

Project Title: The Effects of Composition and Primary Processing on the Microstructure and Mechanical Properties of High-Strength Aluminum Alloys

Project No: E-19-629

Project Director: Dr. T. H. Sanders, Jr.

Sponsor: Naval Air Systems Command; Washington, D.C. 20361

Agreement Period: From 9/29/80 Until 9/28/81 (Perf. Period)

Type Agreement: Contract No. N00019-80-C-0491

Amount: $49,684

Reports Required: Quarterly Progress Report; Transparencies; Final Technical Report

Sponsor Contact Person (s):

Technical Matters

Mr. Michael Valentine
Naval Air Systems Command
Washington, D.C. 20361

Contractual Matters
(thru OCA)

Mr. Thomas A. Bryant
ONR Resident Representative
Georgia Institute of Technology
206 O'Keefe Building
Atlanta, GA 30332

Defense Priority Rating: DO-C9 udner DMS Reg. 1

Assigned to: Chemical Engineering (School/~~Laboratory~~)XXXXXXXX

COPIES TO:

Project Director
Division Chief (EES)
School/Laboratory Director
Dean/Director—EES
Accounting Office
Procurement Office
Security Coordinator (OCA)
Reports Coordinator (OCA)

Library, Technical Reports Section
EES Information Office
EES Reports & Procedures
Project File (OCA)
Project Code (GTRI)
Other OCA Research Property Coordinator

GEORGIA INSTITUTE OF TECHNOLOGY OFFICE OF CONTRACT ADMINISTRATION

SPONSORED PROJECT TERMINATION SHEET

Date 3/7/83

Project Title: The Effects of Composition & Primary Processing on the Microstructure and Mechanical Properties of High-Strength Aluminum Alloys

Project No: E-19-629

Project Director: Dr. T. H. Sanders

Sponsor: Naval Air Systems Command

Effective Termination Date: 9/28/81

Clearance of Accounting Charges: 11/28/81

Grant/Contract Closeout Actions Remaining:

- [ ] Final Invoice and Closing Documents
- [ ] Final Fiscal Report
- [x] Final Report of Inventions
- [ ] Govt. Property Inventory & Related Certificate
- [ ] Classified Material Certificate
- [ ] Other _____

Assigned to: Chemical Eng. (School/~~Laboratory~~)

COPIES TO:

Administrative Coordinator	Research Security Services	EES Public Relations (2)
Research Property Management	Reports Coordinator (OCA)	Computer Input
Accounting	Legal Services (OCA)	Project File
Procurement/EES Supply Services	Library	Other Sanders

FORM OCA 10:781

PROGRESS LETTER REPORT
January 20, 1981

PHASE I--THE EFFECT OF COPPER CONTENT AND FORGING TEMPERATURE ON THE MICROSTRUCTURE OF AN Al-Zn-Mg-Zr ALLOY

Submitted to
Naval Air Systems Command

By
T. H. Sanders, Jr.
Principal Investigator
Fracture and Fatigue Research Laboratory
Georgia Institute of Technology
Atlanta, GA 30332

INTRODUCTION

The general goal of this program is to quantify the effects of composition and processing of Al-Zn-Mg-Cu alloys on the microstructure and to develop quantitative relationships between microstructure and properties. This portion of the program will concentrate on the effects of copper, the processing variable-temperature on the grain structure, and precipitate morphology in a series of hot worked Al-Zn-Mg-Cu alloys.

THEORY

Recovery and Recrystallization

One important feature of hot worked precipitation hardenable aluminum alloys is the tendency to recrystallize during solution heat treatment. The presence of a recrystallized structure can have a dramatic effect on such properties as toughness and corrosion. The tendency toward recrystallization can be controlled by composition and fabrication. However, the details are not perfectly understood and the current theories serve only as a qualitative guide. A quick review of the current understanding of the development of hot worked microstructures is perhaps in order.

Many investigators[1-7] in an effort to quantify the hot working process have observed that temperature (T) and strain rate ($\dot{\varepsilon}$), and the flow stress of the material (σ_ε), can be equated through the relationship:

$$\sigma_\varepsilon = f(Z), \text{ where } Z = \dot{\varepsilon} \exp \frac{\Delta H}{RT},$$

where ΔH is an activation energy, R has its usual meaning, and Z is the Zener-Holloman parameter. The mean strain rate can be estimated by a number of analytic expressions which describe the hot working processes of extrusion, forging and rolling. The temperature can be monitored through the process. Thus, the two variables $\dot{\varepsilon}$ and T can be combined through an equation which relates flow stress to a single experimental parameter, Z, the temperature compensated strain rate.

During the hot working of single phase materials which dynamically recover, a number of microstructural observations have been made. In the initial stages of deformation at a particular temperature compensated strain rate, (Z), dislocations accumulate in tangles. With increasing deformation, the dislocations form boundaries separating regions of low dislocation density. Accompanying the increase in dislocation density, there is a corresponding increase in the flow stress of the material. Eventually, a minimum cell dimension and a constant flow stress are reached, the so called steady state of hot working. The development of a steady state microstructure is a result of dislocation generation and annihilation, with new subgrains of similar dimensions appearing and disappearing as the working process continues.

If the deformation process is carried out at a comparatively low temperature compensated strain rate, the limiting subgrain size is large and the flow stress is low. Conversely, if the temperature compensated strain rate is high, the limiting subgrain size is small and the flow stress high. Thus an inverse correlation of subgrain size with temperature compensated strain rate results.

The basic assumptions in this argument are that during hot working the structural rearrangements occur by thermally activated events and the structure that develops depends principally on the temperature and strain rate.

These observations have been verified numerous times and the mechanism successfully explains the development of structure and the dependence of flow stress on temperature compensated strain rate in high stacking fault energy materials. The same model has been used to predict the behavior of complex alloys. However, a recent investigation[9] has shown that this model is inappropriate in explaining the behavior of commercial, high strength aluminum alloys. Consequently an alternative model has been proposed.

The alternative model recognizes not only the effect of Z on structure but the effect of the presence of particles of a second phase and their modification on the development of the hot worked structure. In high strength aluminum alloys, there are three types of precipitates present: i.e., secondary intermetallics, dispersoids, and equilibrium precipitates of the major solute elements which precipitate at the hot working temperatures.

Numerous investigations have shown the effect of secondary intermetallics on the static recrystallization process. These coarse, non-deformable particles tend to localize deformation in the vicinity of the particle/matrix interface during hot working. Consequently, these areas of high dislocation density act as sites for recrystallization during solution heat treatment.

The dispersoids and the equilibrium precipitates of the major solute elements are finer (between 0.2 μm to 0.5 μm) and more uniformly distributed throughout the material than are the secondary intermetallics. During hot working these particles also act as sources for the generation of dislocations.

The average spacing of these precipitates is on the order of 1-5 μm depending on composition and fabricating soak temperature. The subgrain size is a function of this spacing only and is independent of Z[9]. Rather than the temperature compensated strain rate determining the number and distribution of operative dislocation sites, Z determines the number of dislocations generated by a particular site. Thus, as observed in a recent study, the subgrain misorientation appears to be qualitatively related to Z. Increasing Z increases the misorientation.

Using this model, one can explain the recrystallization behavior of high strength alloys upon solution heat treatment. With increasing Z there is an increase in the number of dislocations generated at a source. During working the dislocations rearrange themselves into low angle boundaries. The angle of the boundary increases with increasing number of dislocations. Thus with increasing Z there is a concomitant increase in the misorientation of the subgrain boundaries. A boundary with a high misorientation can act as a nucleus for recrystallization. Upon solution heat treatment, two events which affect recrystallization are occurring. First, the elevated temperature supplies the energy for subgrain boundary migration. Second, at the solution heat treatment temperature the precipitates of the major solute elements are dissolving. Thus reducing their effectiveness to retarding boundary migration. The dispersoids then must act as barriers to pin the advancing front. At a high Z, for example, the driving force for recrystallization may be sufficiently high that the dispersoids are ineffective at retarding recrystallization.

This phase of the investigation is to determine the effect of copper content and hot forging temperature on the substructure of a variety of Al-Zn-Mg-Cu alloys, and determine if the tendency to recrystallize can be related to substructure.

EXPERIMENTAL

Table 1 contains a summary of the chemical compositions of eight Al-Zn-Mg-Zr alloys being investigated in the first phase of this program.

Heat Treatment

Specimens 1.9 cm (.75") thick, 5.1 cm (2.0") wide, and 12.7 cm (5.0") long were two step preheated (4 hours at 733K (860°F) followed by 16 hours at 750K (890°F)) in an ammonium fluoroborate atmosphere. The specimens were then reheated for one hour to their respective forging temperature. Table 2 summarizes the forging temperatures used.

Forging

The specimens were upset forged in the thickness direction to approximately ½ their original thickness. Immediately after forged sections were quenched in cold water. Sections for metallography, x-ray pinhole, and transmission electron microscopy (TEM), have been prepared.

ANTICIPATED WORK FOR NEXT QUARTER

The metallographic and x-ray analysis will be completed to determine the effects of forging temperature and composition on the tendency to recrystallize in the as-forged, forged, and solution heat treated specimens. The correlation between probability to recrystallize and substructure will be completed.

REFERENCES

1. B. J. Meadows, M. J. Cutler, Journal of the Institute of Metals, 97, (1969), 321.

2. T. Sheppard and D. Raybould, ibid., 101, (1973), 33.

3. D. Raybould and T. Sheppard, ibid., 101, (1973), 45.

4. D. Raybould and T. Sheppard, ibid., 101, (1973), 65.

5. T. Sheppard and D. Raybould, ibid., 101, (1973), 73.

6. M. M. Faray and M. H. Ahmed, Materials Science and Engineering, 17, (1965), 131.

7. M. M. Faray and C. M. Sellars, Metals Technology, 172, (1975), 220.

8. J. T. Staley and R. R. Sawtell, "Alloy 7050 Extrustions," presented at Western Tool Exposition and Metal Congress (WESTEC) Los Angeles, CA, March 14-17, 1977.

9. T. H. Sanders, Jr., "Improving Fatigue Resistance of Naval Aircraft Alloys," Naval Air Systems Command, Final Report. (In progress).

TABLE 1. Composition of the Alloys in Phase 1
(weight per cent)

Cu	Zn	Mg	Fe	Si	Zr	Al
0.04	6.35	2.28	0.13	0.06	0.12	Balance
0.44	6.50	2.32	0.13	0.05	0.13	"
1.11	6.50	2.30	0.14	0.06	0.12	"
1.44	6.62	2.32	0.14	0.06	0.13	"
1.74	6.62	2.37	0.14	0.06	0.12	"
1.67	6.45	2.26	0.14	0.06	0.13	"
2.13	6.58	2.34	0.15	0.06	0.13	"
2.41	6.56	2.34	0.17	0.06	0.13	"

TABLE 2. Forging Temperatures

Temperature (°C)	Lubricant
225	Polypropylene
275	"
325	"
375	PL493
425	"

PROGRESS LETTER REPORT
April 29, 1981

PHASE I--THE EFFECT OF COPPER CONTENT AND FORGING TEMPERATURE ON THE MICROSTRUCTURE OF AN Al-Zn-Mg-Zr ALLOY

Submitted to
Naval Air Systems Command

By
T. H. Sanders, Jr.
Principal Investigator
and
S. B. Chakrabortty
Research Scientist
Fracture and Fatigue Research Laboratory
Georgia Institute of Technology
Atlanta, GA 30332

INTRODUCTION

This phase of the investigation is to determine the effect of copper content and hot forging temperature on the substructure of a variety of Al-Zn-Mg-Cu alloys, and determine if the tendency to recrystallize can be related to substructure.

EXPERIMENTAL

Table 1 contains a summary of the chemical compositions of eight Al-Zr-Mg-Zr alloys being investigated in the first phase of this program.

Heat Treatment

Specimens 1.9 cm (.75") thick, 5.1 cm (2.0") wide, and 12.7 cm (5.0") long were two step preheated (4 hours at 733K (860°F) followed by 16 hours at 750K (890°F)) in an ammonium fluoroborate atmosphere. The specimens were then reheated for one hour to their respective forging temperature. Table 2 summarizes the forging temperatures used.

Forging

The specimens were upset forged in the thickness direction to approximately ½ their original thickness. Immediately after deformation the forged sections were quenched in cold water.

Microstructure

The microstructures of the various alloys were examined in the as-forged (F-temper) and solution heat treated (W-temper) conditions. The SHT was carried out at 490°C in molten salt for ½ hour. The samples were then cold water quenched. Particular F-temper samples were examined using the transmission electron microscope (TEM). Wafers approximately 0.5 mm thick were sectioned from the forging and discs 3 mm in diameter were punched from the wafers. The discs were electropolished using a twin jet polishing technique in a 3:1-methanol:nitric acid solution cooled to -36°C. The foils were examined in a JEOL-JEM 100C electron microscope.

Optical microscopy was conducted on selected W-temper material. The samples were mounted in bakelite, mechanically polished and anodized in a solution containing 948 ml H_2O, 55 ml HBF_4 and 7 grams H_3BO_4 at 18 volts d.c. The samples were examined using polarized light.

Tensile Tests

Duplicate LT-tensile specimens were machined from SHT, quenched, and aged (24 hours at 120°C) blanks from the copper free and maximum copper alloys (Table 1) forged at the lowest and highest temperatures (Table 2).

Texture (Preferred Orientation) Characterization

The development of polycrystalline grain preferred orientation due to casting, forging and SHT is under investigation with X-ray diffraction texture analysis. The method of texture analysis is based on the Schultz diffractometer method and a Siemens automated texture goniometer is used. Texture data are plotted on a stereographic projection with iso-intensity lines drawn for certain multiples of the random intensity.

A complete determination of crystallographic texture is being conducted using the (111), (200), and (220) pole figures. The complete pole figures are obtained from specimens which are cut from stacked plates following the method of Meiran[1] and Lopata.[2] The texture studies are being conducted on low and high copper alloys forged at the lowest and highest temperatures. The measurements are being made on F- and W- temper materials.

RESULTS

Microstructure

Figure 1 shows samples of the low copper alloy forged at 225 and 425°C. Only at the highest temperature (425) was barrelling observed. At the other four temperatures (225, 275, 325 and 375°C) the lubricant was affective, and the rectangular shape of the starting section was maintained.

Figures 2-4 contain TEM micrographs showing the precipitate morphology, subgrain structure, and dislocation distribution for particular F-temper microstructures. Figure 5 contains polarized light micrographs of low and high copper forged at 225 and 425°C, SHT at 490° for 0.5 hours and cold water quenched.

From these and other micrographs the following set of observations can be made:

1. At a particular forging temperature increasing the copper content increases the probability to recrystallize after SHT.
2. Decreasing the forging temperature increases the probability to recrystallize after SHT.
3. Composition and forging temperature have a profound effect on the forged microstructure. Increasing the composition increases the amount and type of equilibrium phase present at a particular forging temperature.
4. There are two types of equilibrium precipitates: M($MgZn_2$) an S (Al_2CuMg). As the copper content increases, the amount of S phase present increases. Decreasing the forging temperature increases the amount of equilibrium precipitates.
5. At a given forging temperature, increasing the copper content increases the regularity of the subgrain structure. Furthermore, increasing the temperature for a particular composition increases the regularity of the substructure.

Mechanical Properties

The tensile properties for the low and high copper alloys forged at 225 and 425°C are summarized in Table 3.

FUTURE WORK

The quantitative relationship between forging temperature, composition and SHT microstructure will be completed. A separation of the influence of equilibrium precipitates and deformation temperature will be attempted during this quarter. The influences of microstructure and composition on quench sensitivity will be completed. The detailed texture analysis will be completed and related to the other microstructural studies.

ACKNOWLEDGMENTS

Texture studies are being conducted by Dr. S. Spooner

REFERENCES

1. E. S. Meiron, Rev. Sci. Instr., 33:319-322 (1962)

2. S. L. Lpata and E. B. Kula, Trans. AIME, 224:865-866 (1962)

TABLE 1. Composition of the Alloys in Phase 1
(weight per cent)

Cu	Zn	Mg	Fe	Si	Zr	Al
0.04	6.35	2.28	0.13	0.06	0.12	Balance
0.44	6.50	2.32	0.13	0.05	0.13	"
1.11	6.50	2.30	0.14	0.06	0.12	"
1.44	6.62	2.32	0.14	0.06	0.13	"
1.74	6.62	2.37	0.14	0.06	0.12	"
1.67	6.45	2.26	0.14	0.06	0.13	"
2.13	6.58	2.34	0.15	0.06	0.13	"
2.41	6.56	2.34	0.17	0.06	0.13	"

TABLE 2. Forging Temperatures

Temperature (°C)	Lubricant
225	Polypropylene
275	"
325	"
375	PL493
425	"

TABLE 3. Yield Strength Dependence on Composition and Forging Temperature

	Forging Temperature 225°C	425°C
Low Copper (0.04 Cu)	473 MPa 446 MPa Avg = 460 MPa	507 488 Avg = 498 MPa
High Copper (2.41 Cu)	507 MPa 499 MPa Avg = 503 MPa	589 MPa 553 MPa Avg = 571 MPa

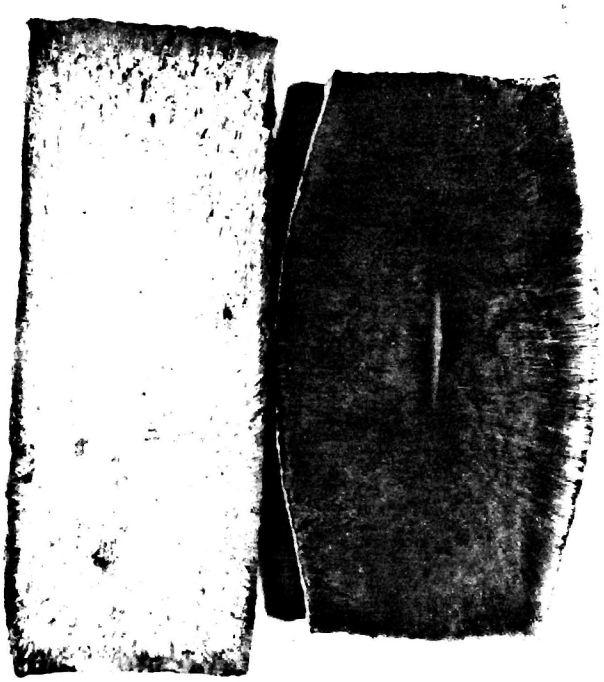

Figure 1. Photograph showing representative samples forged at 225 and 425°C

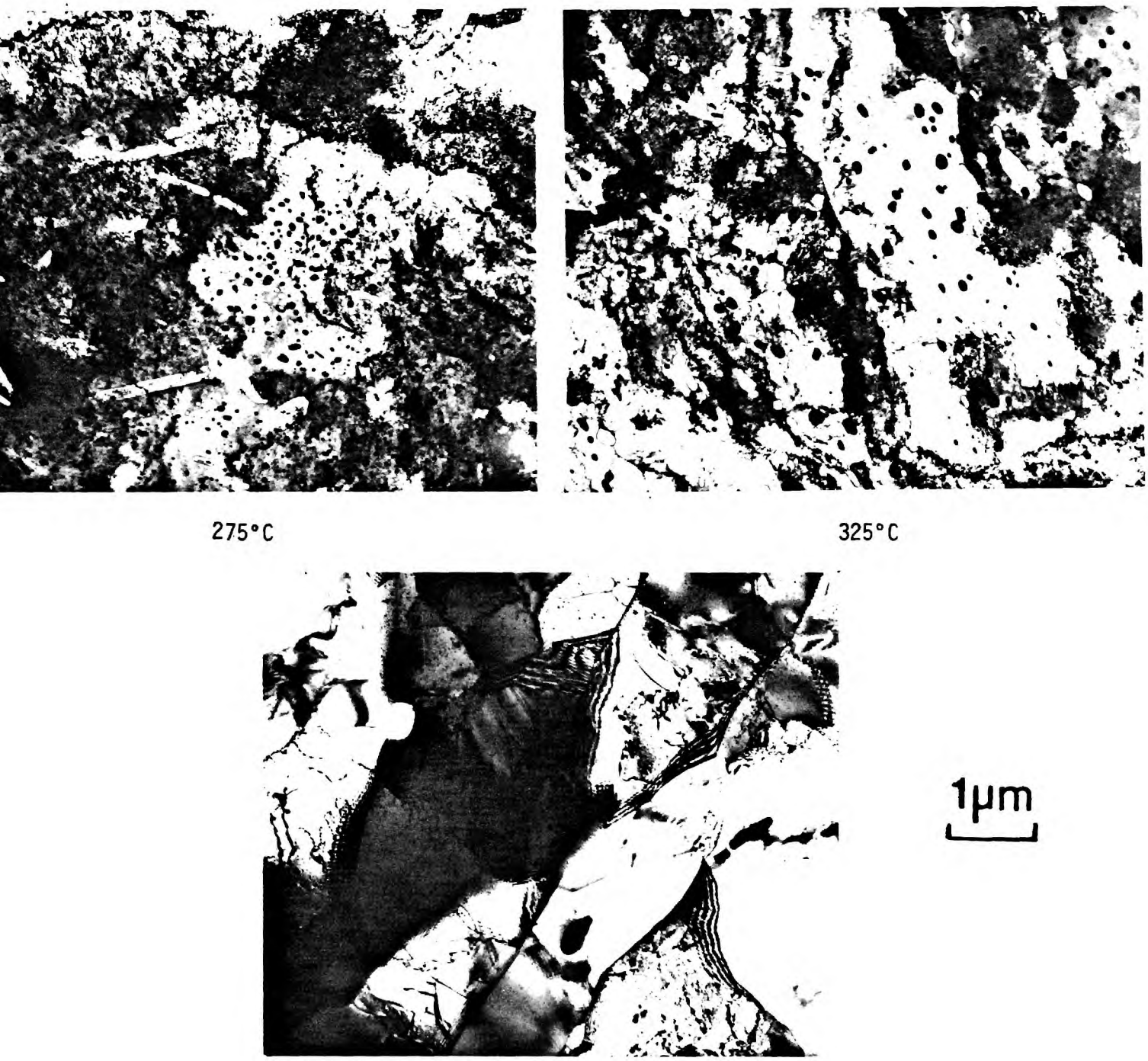

Figure 2. Representative TEM's illustrating the effect of forging temperature on substructure of the low copper alloy.

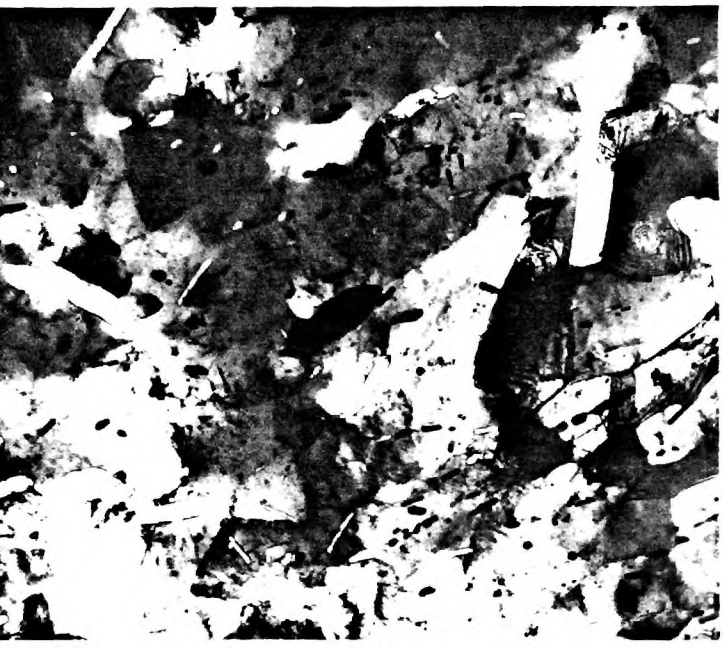

275°C

325°C

375°C

1μm

Figure 3. Representative TEM's illustrating the effect of forging temperature on substructure of the high copper alloy.

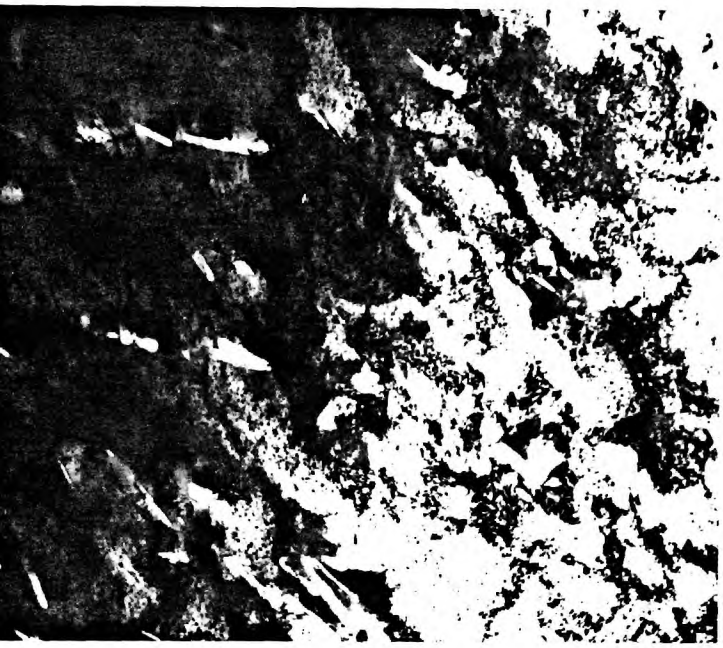

0.44 Cu

1.44 Cu

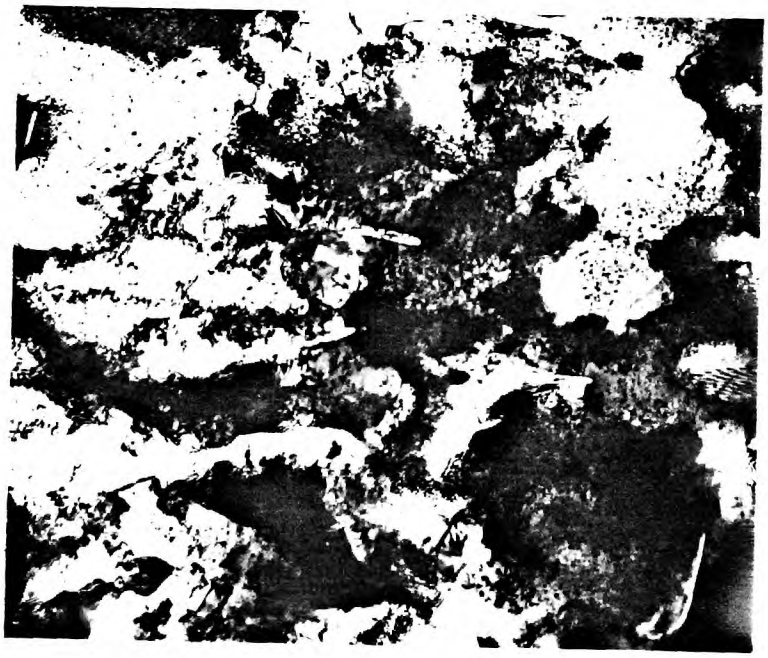

1μm

1.67 Cu

Figure 4. The effect of composition on precipitate morphology and substructure on three alloys forged at 225°C.

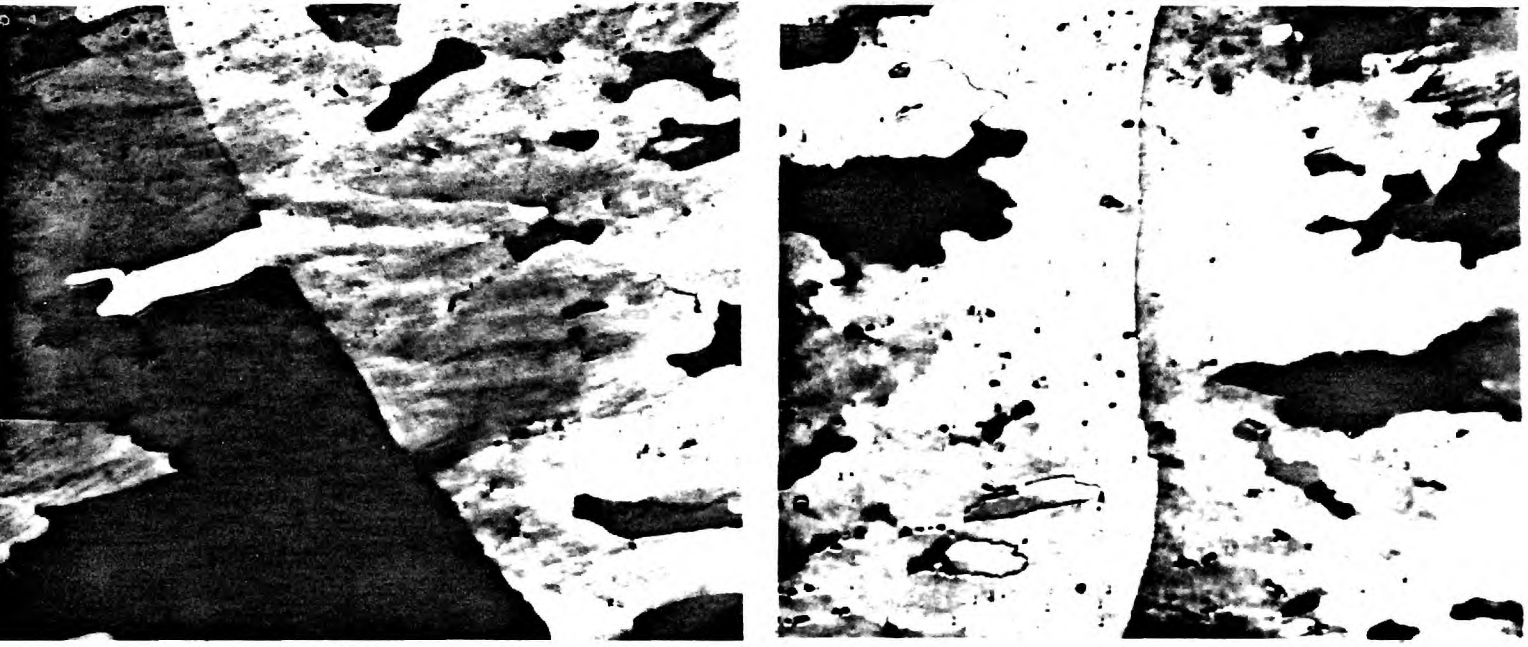

0.04 Cu
425°C

2.41 Cu
425°C

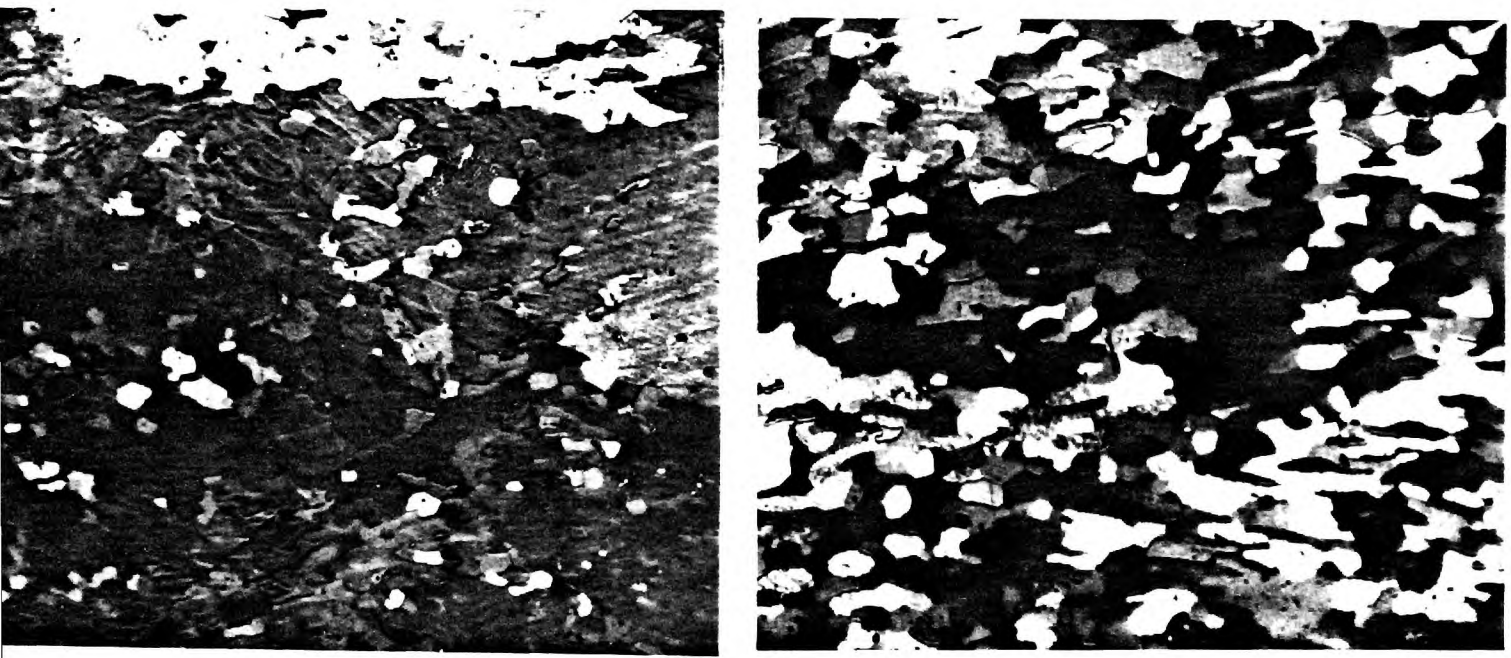

0.04 Cu
225°C

2.41 Cu
225°C

100 μm

Figure 5. Polarized light micrographs illustrating the effect of forging temperature and copper content on the grain structure after solution heat treatment. Longitudinal section.

PROGRESS LETTER
August 10, 1981

THE INFLUENCE OF INGOT STRUCTURE COMPOSITION AND HOT WORKING ON THE MICROSTRUCTURE OF Al-Zn-Mg-Cu-Zr ALLOYS

Submitted to
Naval Air Systems Command

By
T. H. Sanders, Jr.
Principal Investigator
Fracture and Fatigue Research Laboratory
Georgia Institute of Technology
Atlanta, Georgia 30332

INTRODUCTION

The general goal of this program is to quantify the effects of starting microstructure, composition, and processing conditions (temperature and strain rates) on the wrought microstructure.

EXPERIMENTAL

Table 1 contains a summary of the chemical compositions of the eight Al-Zn-Mg-Cu-Zr alloys being investigated in this program.

HEAT TREATMENT

Specimens 1.9 cm (.75") thick, 5.1 cm (2.0") wide, and 12.7 cm (5.0") long were two step preheated (4 hours at 733K (860°F) followed by 16 hours at 750K (890° F) in an ammonium fluoroborate atmosphere. The specimens were then reheated for one hour to their respective hot working temperatures. Table 2 summarizes the forging temperatures used.

FORGING

Table 2 summarizes the forging temperatures used. The specimens were upset forged in the thickness direction to approximately ½ their original thickness. Immediately after deformation the forged sections were quenched in cold water.

ROLLING

Orientation Effects: To determine the effect of starting ingot orientation, preheated ingots were rolled parallel and perpendicular to the casting direction. Alloys 70A and 71D (Table 1) were used for this investigation. The preheated ingots were reheated to 375°C and hot rolled approximately 10% per pass, the ingots were reheated between each pass. The final thickness (1 cm) was approximately 50% of the starting thickness (1.9 cm). Sections for metallographic examination and texture determination were cut from each rolled plate.

The plates were then further rolled at 300°C to 0.5 cm in two passes. The plates were reheated between passes. Sections for metallographic examination and texture determination were cut from each rolled plate.

Temperature Effects: To separate the influence of rolling temperature on solubility of the major elements from effect of temperature on the deformation, alloy 71D was hot rolled at 300° using two schemes. Two ingots were SHT at 490°C, and cold water quenched. One ingot was reheated for 24 hours at 300°C and the other was immersed in molten lead-antimony eutectic for five minutes. The alloys were rolled 20%, 20%, and 50%. The plates were reheated in the molten metal for 2 minutes between each pass. Sections were prepared for metallograhic examination.

COLD ROLLING

Pieces of each forged alloy were SHT, CWQ, and reheated to 300°C for 24 hours, then cold rolled to 0.1 cm to achieve a fully recrystallized fine grain structure.

AGING KINETICS

The effect of composition on the second step aging kinetics were determined by following changes in hardness. The alloys were SHT at 490°C, CWQ, aged 24 hours at 120°C and different times at 140, 160, 170 and 180°C.

MICROSTRUCTURE

The microstructures of the various alloys were examined in the as-forged (F-temper) and solution heat treated (W-temper conditions. The SHT was carried out at 490°C in molten salt for ½ hour. The samples were then cold water quenched. Particular F-temper samples were examined using the transmission electron microscope (TEM). Wafers approximately 0.5 mm thick were sectioned from the forging and discs 3 mm in diameter were punched from the wafers. The discs were electropolished using a twin jet polishing technique in a 3:1-methanol:nitric aicid

solution cooled to -36°C. The foils were examined in a JEOL-JEM 100C electron microscope.

Optical microscopy was conducted on selected W-temper material. The samples were mounted in bakelite, mechanically polished and anodized in a solution containing 948 ml H_2O, 55 ml HBF_4 and 7 grams H_3BO_4 at 18 volts d.c. The samples were examined using polarized light.

CORROSION TESTING

Free corrosion potential measurements and potentiodynamic scans were performed on specimens which had been cold rolled, solution heat treated, and artifically aged. A uniform surface preparation was applied to each specimen prior to exposure, the last step of which was fine grinding on a 600 grit water cooled silicon carbide abrasive disc. The electrolyte used in all of the experiments was a 3.5 weight percent NaCl solution prepared using distilled water. The electrolyte temperature during all of the experiments was maintained at 25°C.

Free Corrosion Potential Measurements: The corrosion potential (vs. SCE) of specimens in a stirred solution open to lab air was recorded immediately after immersion, and after 24 hours of exposure.

Potentiodynamic Scans: Specimen electrodes were prepared with a cm^2 surface area exposed to the electrolyte. A scan generator was used to set the start potential (in the cathodic region), scan rate (10 and 2 mV/min) and the scan range (typically extending past the breakdown potential). The potentiostat drove the electrode initially as a cathode, which provides a certain amount of surface cleaning, and normalizes the specimen, continued through the zero current potential, and into the anodic region. Current passing through the specimen was recorded as a function of impressed potential, using an X-Y recorder.

EXPERIMENTAL RESULTS

As-Cast Microstructure

The alloys being investigated in this program contain twin columnar grains (TCG). Figure 1 shows a polarized light optical micrograph taken of alloy 70A showing the cast grain structure. A large thermal gradient ahead of the solid-liquid interface facilitates the formation of the twin structure.

The Crystallography of TCG

The <100> direction of growth is the usual growth direction for dendrites in aluminum. There are two possibilities that might explain this observation. In one, the process of atomic attachment is kinetically favored on the {100} surface. Alternatively, the geometry of the tip of a dendrite arm would be favorable for diffusion of heat or solute atoms when it grows in the <100> direction because of anisotropy in surface energy. Since the closed pack {111} surfaces have the longest surface energy and since the [100] direction is surrounded by four {111} planes, this then results in a growth tip in the [100] direction if geometry is controlled by surface energy. Figure 2 illustrates the geometry of a regular figure composed of {111} surface planes. A stereographic projection is included to show the planes involved.

Figure 3 illustrates the effect of twinning across the (111) plane. What results is a polygon having 14 sides, all of which are {111} planes. This time the direction of growth is a <112> and it is surrounded by 6 {111} planes.

Figure 4 is a schematic illustrating the TCG structure in composite. The structure is composed of a series of alternating twins A and B which are separated by a twin boundary (straight line) and a curved boundary.

The process of TCG occurs during solidification. The twin bounary is the first to freeze, and therefore, contains no secondary intermetallic compounds

(i.e., Al_7Cu_2Fe,Mg_2Si, etc.). This point is illustrated in the micrograph in Figure 5.

The major thrust of the last quarter of this program will be to determine the influence of this type of structure on fracture, where recrystallization begins, and how the orientation of these twin boundaries with respect to rolling influences the wrought structure.

Forged Microstructure

From the experiments to date, the following observations can be made:

1. At a particular forging temperature increasing the copper content increases the probability to recrystallize after SHT.
2. Decreasing the forging temperature increases the probability to recrystallize after SHT.
3. Composition and forging temperature have a profound effect on the forged microstructure. Increasing the composition increases the amount and type of equilibrium phase present at a particlar forging temperature.
4. There are two types of equilibrium precipitates: M($MgZn_2$) and S(Al_2CuMg). As the copper content increases, the amount of S phase present increases. Decreasing the forging temperature increases the amount of equilibrium precipitates.
5. At a given forging temperature, increasing the copper content increases the regularity of the subgrain structure. Furthermore, increasing the temperature for a particular composition increases the regularity of the substructure.

Aging Kinetics

The influence of composition and temperature on the second stop aging kinetics are shown in Figures 6-12. These results indicate that increasing

copper content delays the onset of overaging, but once the overaging begins, it occurs more rapidly with increasing copper content.

This last phase of the program will explore the basic mechanisms of overaging in this system and the influence of copper on the structure of η.

Corrosion Investigations

The free corrosion potential, data are summarized in Table 3. The polarization curves will be completed in the last quarter and considered in light of the aging response.

FUTURE WORK

Complete microstructure investigations, texture, corrosion, and write final report.

TABLE 1. Composition of the Alloys in Phase 1
(weight per cent)

ALLOY	Cu	Zn	Mg	Fe	Si	Zr	Al
70 A	0.04	6.35	2.28	0.13	0.06	0.12	Balance
B	0.44	6.50	2.32	0.13	0.05	0.13	"
C	1.11	6.50	2.30	0.14	0.06	0.12	"
D	1.44	6.62	2.32	0.14	0.06	0.13	"
71 A	1.74	6.62	2.37	0.14	0.06	0.12	"
B	1.67	6.45	2.26	0.14	0.06	0.13	"
C	2.13	6.58	2.34	0.15	0.06	0.13	"
D	2.41	6.56	2.34	0.17	0.06	0.13	"

TABLE 2. Forging Temperatures

Temperature	Lubricant
225	Polypropylene
275	"
325	"
375	PL493
425	"

TABLE 3.

FREE CORROSION POTENTIAL MEASUREMENTS

All experiments conducted in 3.5% NaCl, stirred, at 25°C, and exposed to lab air.

I. Specimens recieved were solution heat treated at 490°C for 0.5h,CWQ, then artificially aged at 120°C for 24h.

	70A	70B	70C	70D	71A	71C	71D
0 h	-0.970	-0.926	-0.823	-0.821	-0.792	-0.769	-0.756
24 h	-0.950	-0.825	-0.747	-0.782	-0.739	-0.711	-0.733

Experiment repeated with the following results:

	70A	70B	70C	70D	71A	71C	71D
0 h	-0.970	-0.919	-0.825	-0.806	-0.796	-0.769	-0.757
24 h	-0.930	-0.817	-0.745	-0.827	-0.809	-0.710	-0.704

II. Specimens were solution heat treated, and cold water quenched. Mounting and testing were done as quickly as possible, but some room temperature aging may have taken place.

	70A	70B	70C	70D	71A	71C	71D
0 h	-0.975	-0.942	-0.844	-0.824	-0.812	-0.790	-0.776
24 h	-0.982	-0.951	-0.838	-0.819	-0.807	-0.785	-0.745

III. Specimens were solution heat treated, CWQ, aged 24 h at 120°C, then second step aged at 180°C for various times (see SSA heat treat schedule)

	70A 3	70A 4	71A 1	71A 2	71A 3	71D 1	71D 2	71D 3	71D 4
0 h	-0.950	-0.942	-0.769	-0.762	-0.765	-0.743	-0.744	-0.750	-0.755
24 h	-0.918	-0.856	-0.765	-0.773	-0.777	-0.759	-0.763	-0.770	-0.778

IV. Hardness free corrosion specimens aged so as to achieve equal hardness (DPH 140).

	70A	71A	71D
0 h	-0.920	-0.765	-0.760
24 h	-0.656	-0.759	-0.756

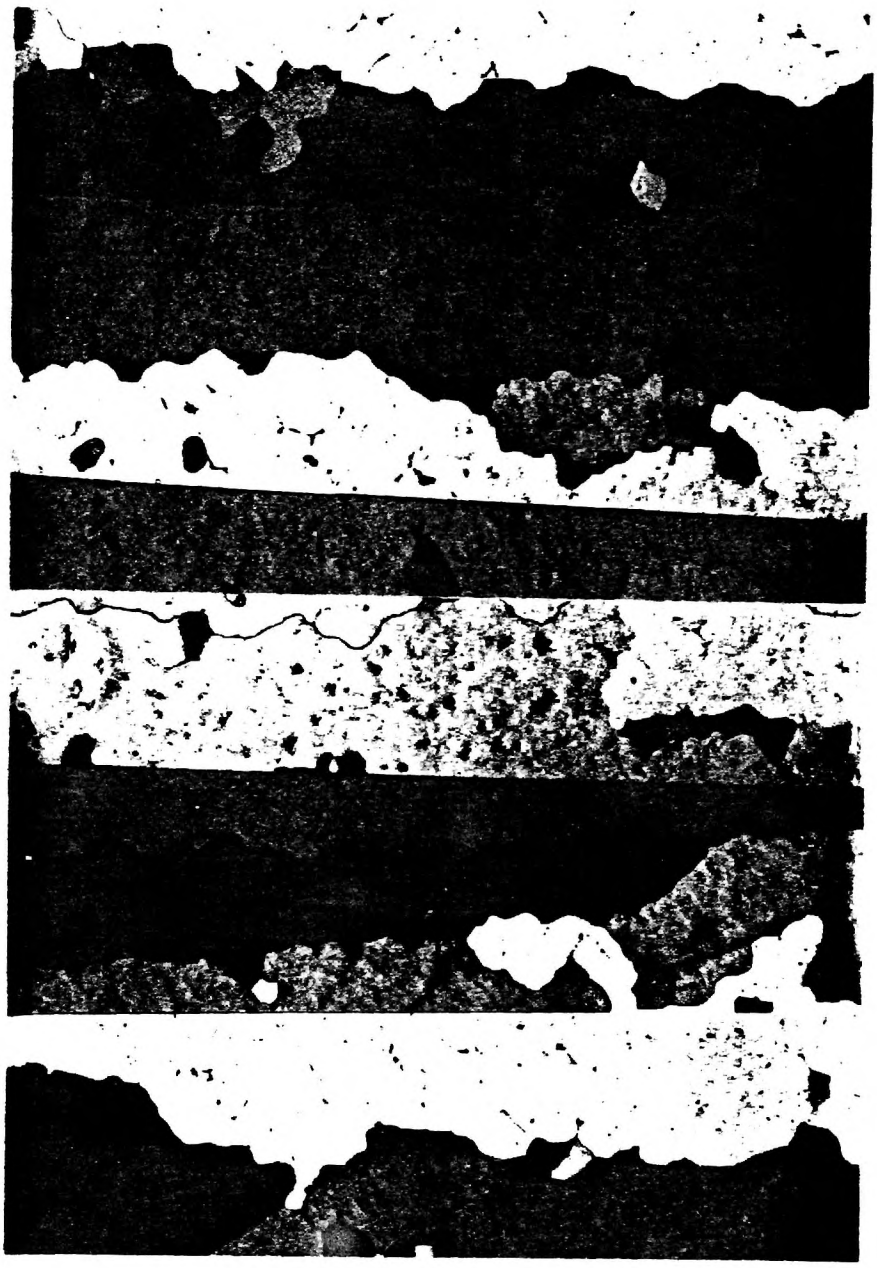

Figure 1. Microstructure showing TCG structure in the as-cast ingot.

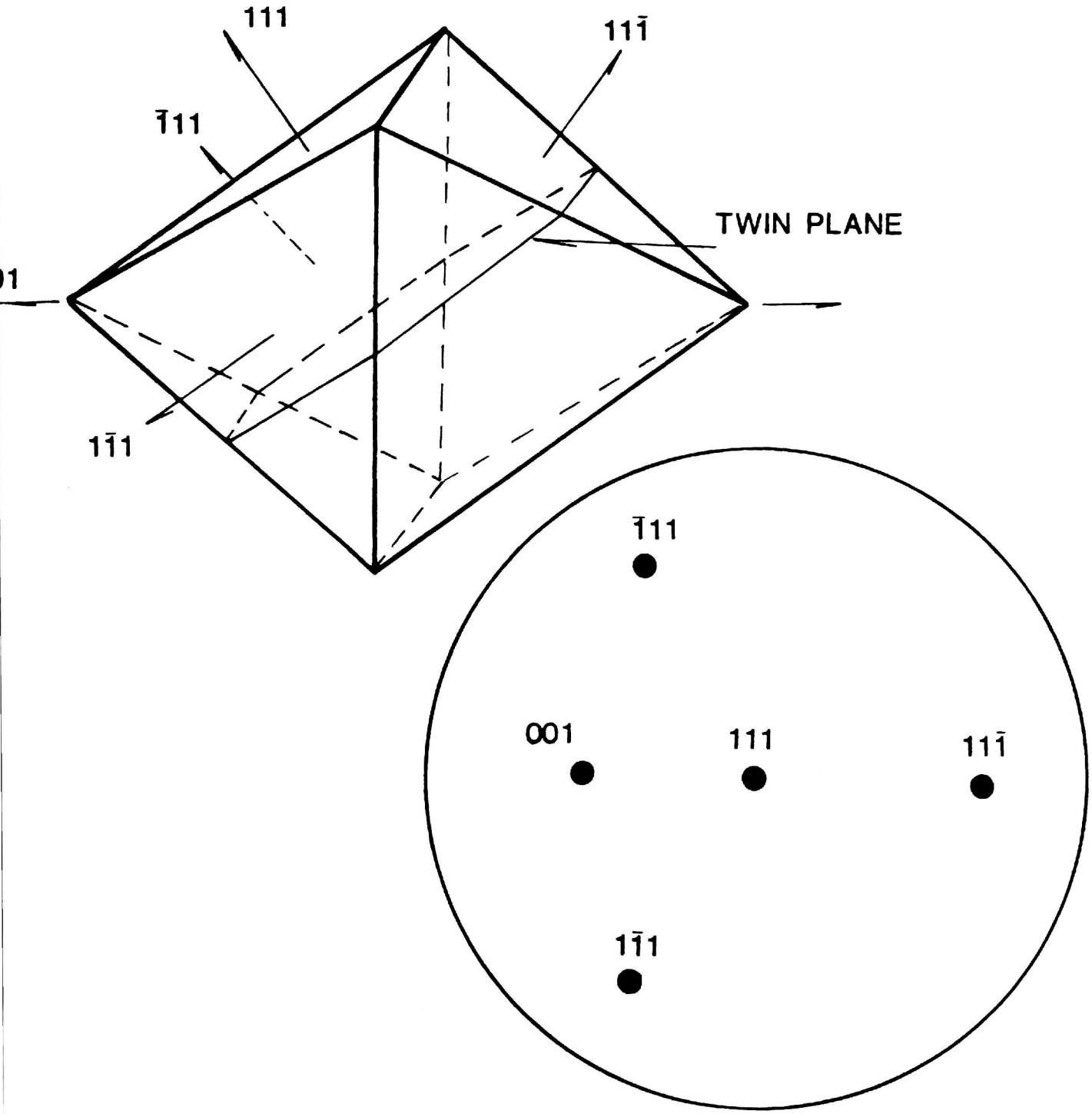

Figure 2. Geometry <100> growth with a high degree of anisotropy.

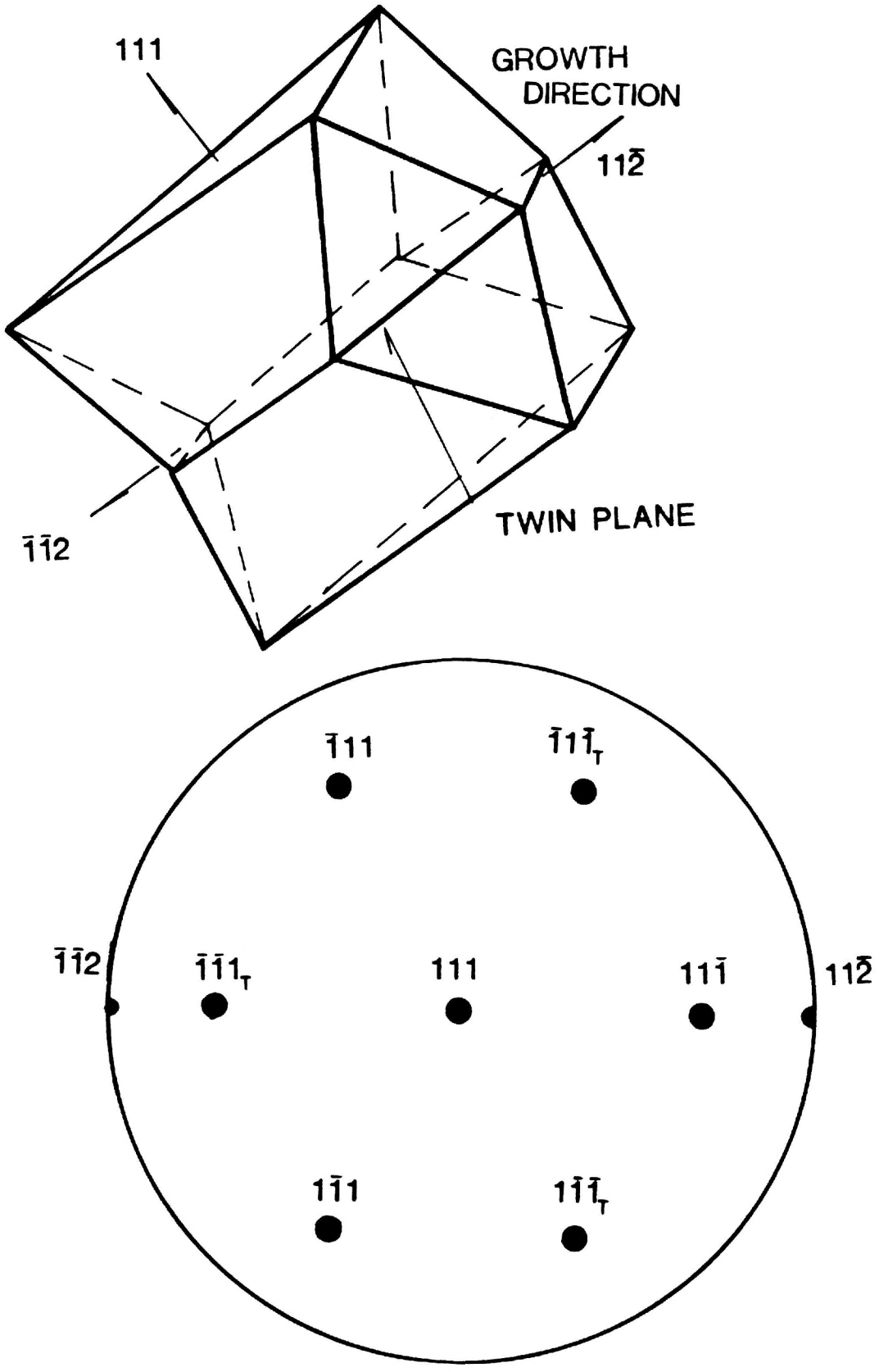

Figure 3. Equilibrium shape after twinning across the (111) plane.

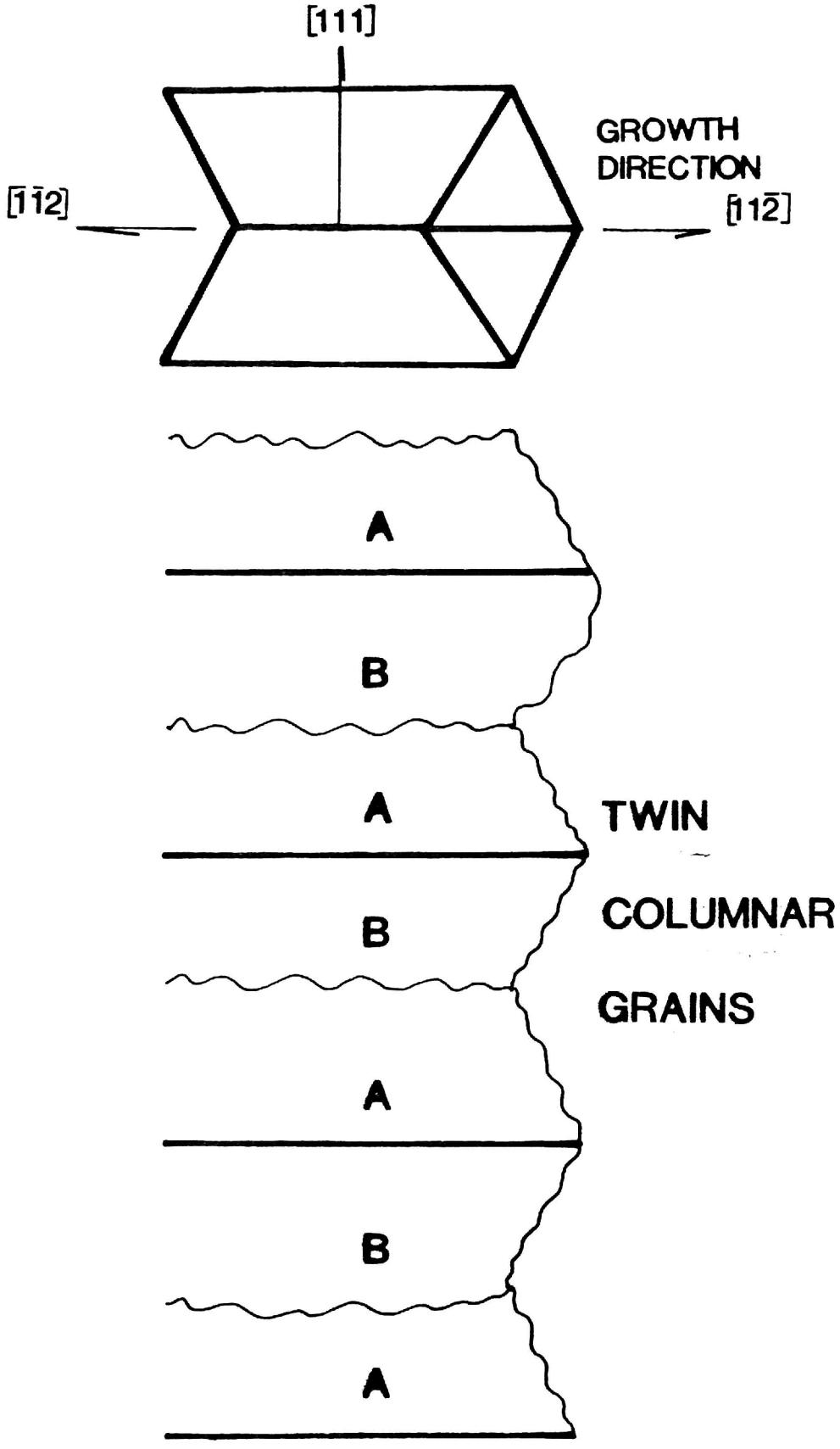

Figure 4. Composite showing alternate A, B twins.

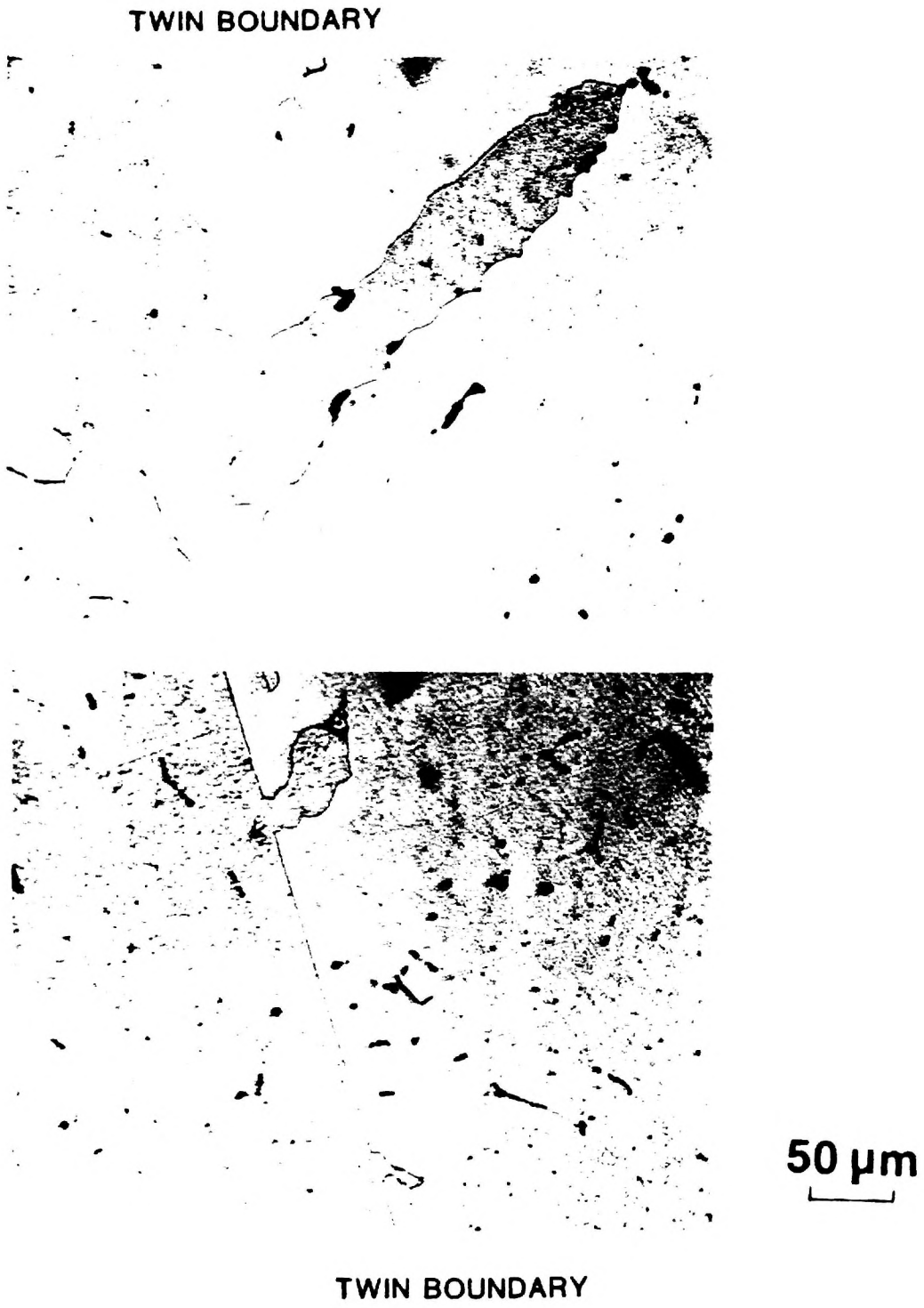

Figure 5. Micrographs of 71D showing the distribution of insolubles in material having TCG.

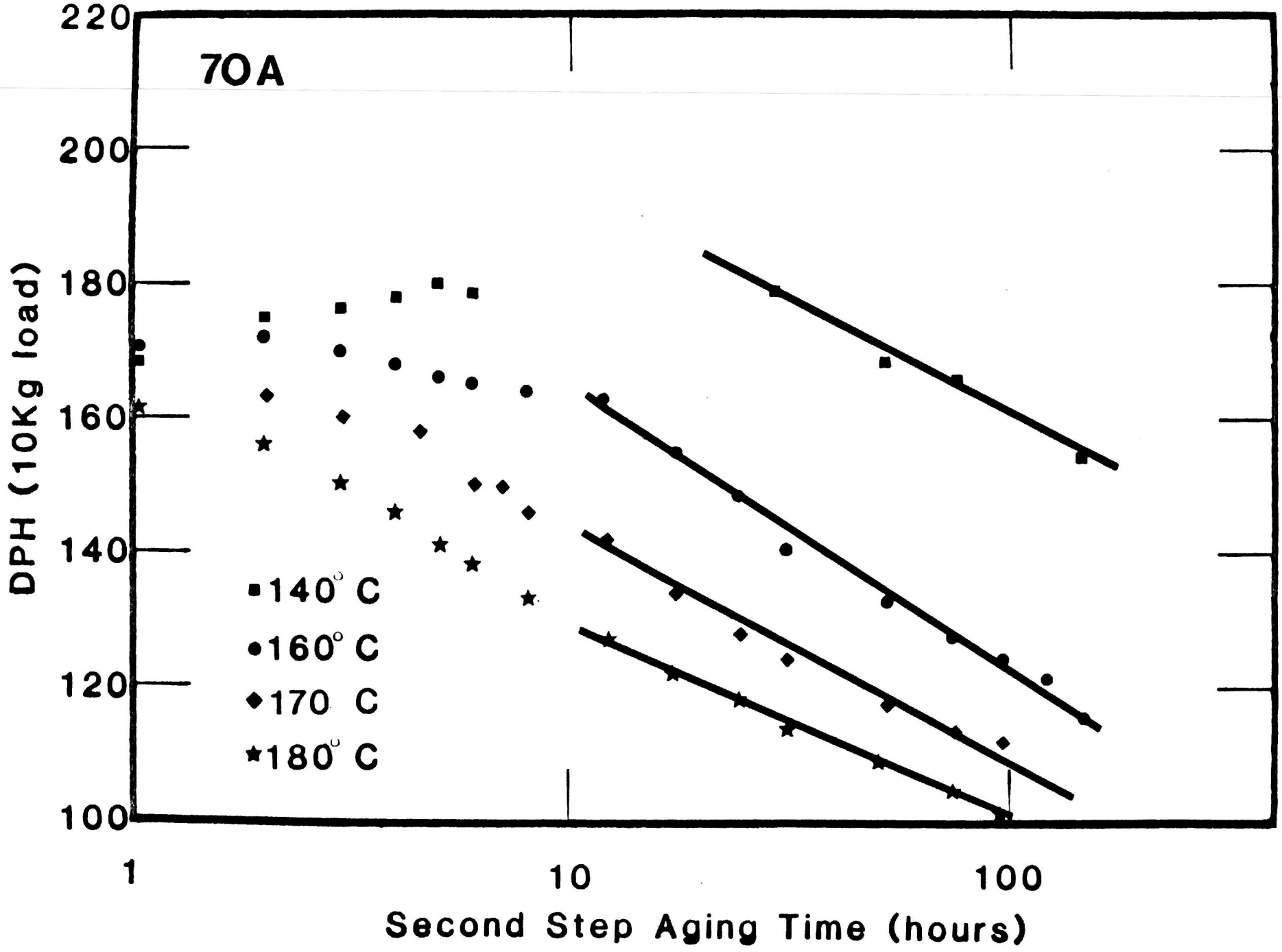

Figure 6. Kinetics of second step aging.

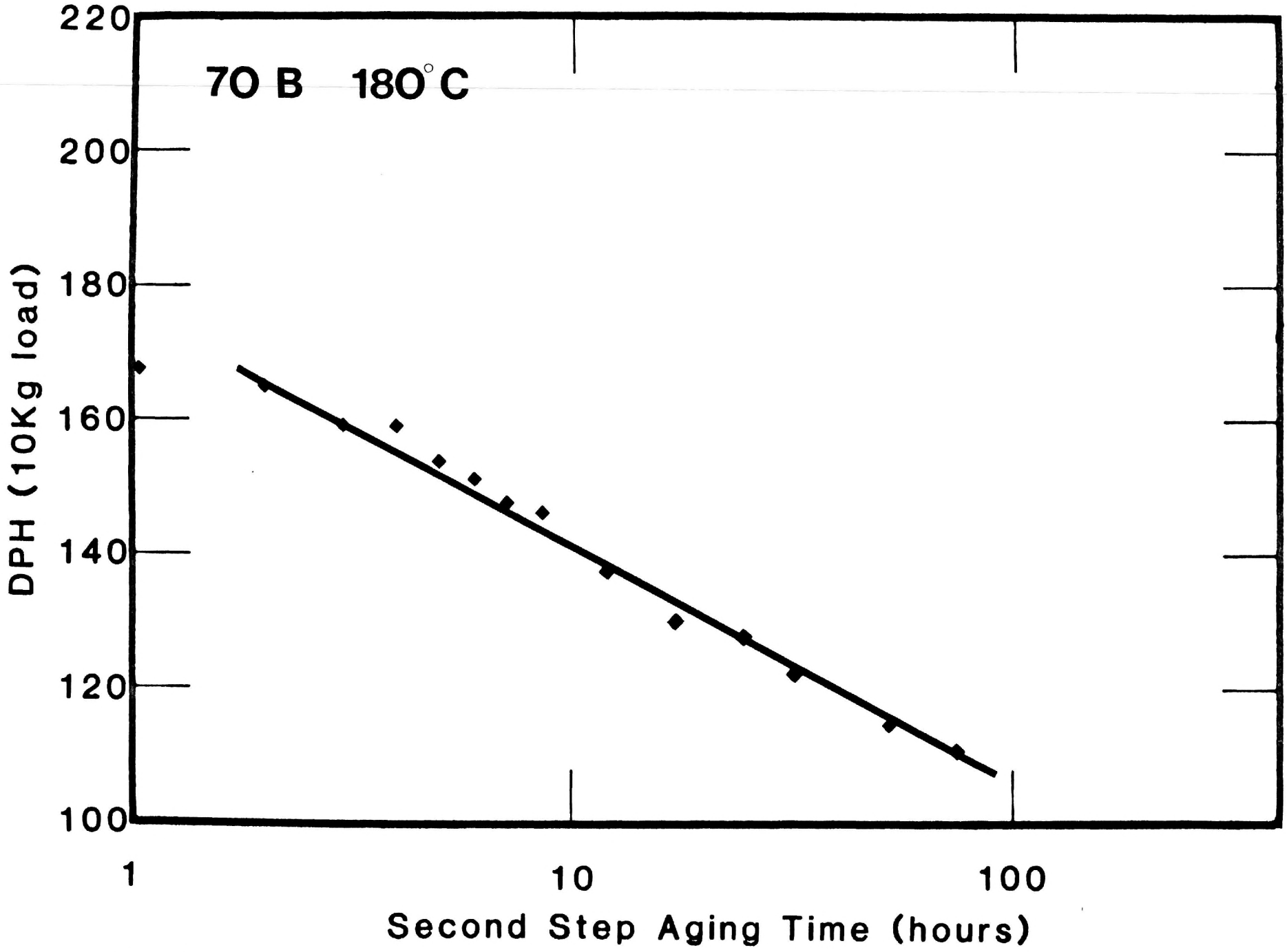

Figure 7. Kinetics of second step aging.

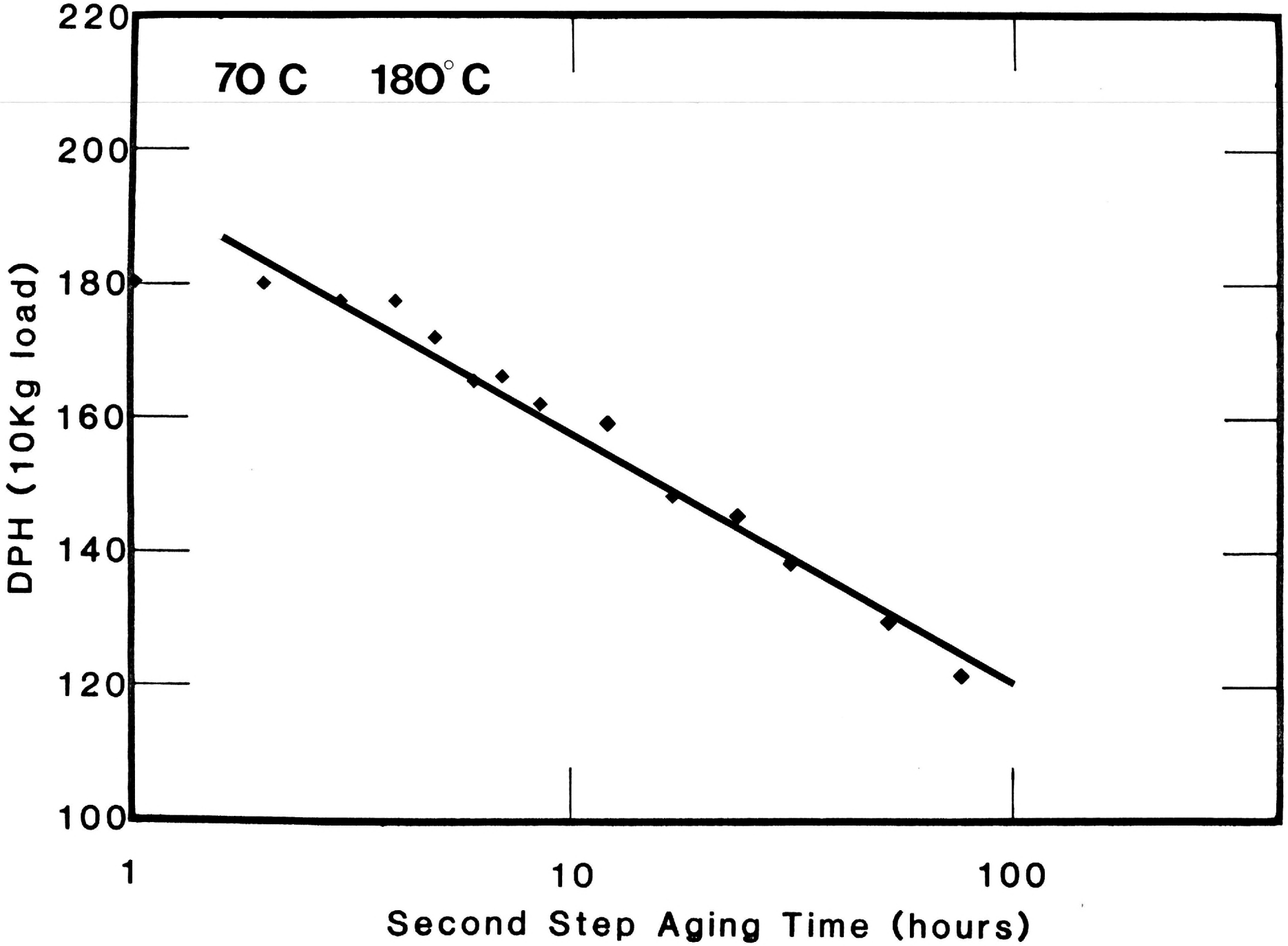

Figure 8. Kinetics of second step aging.

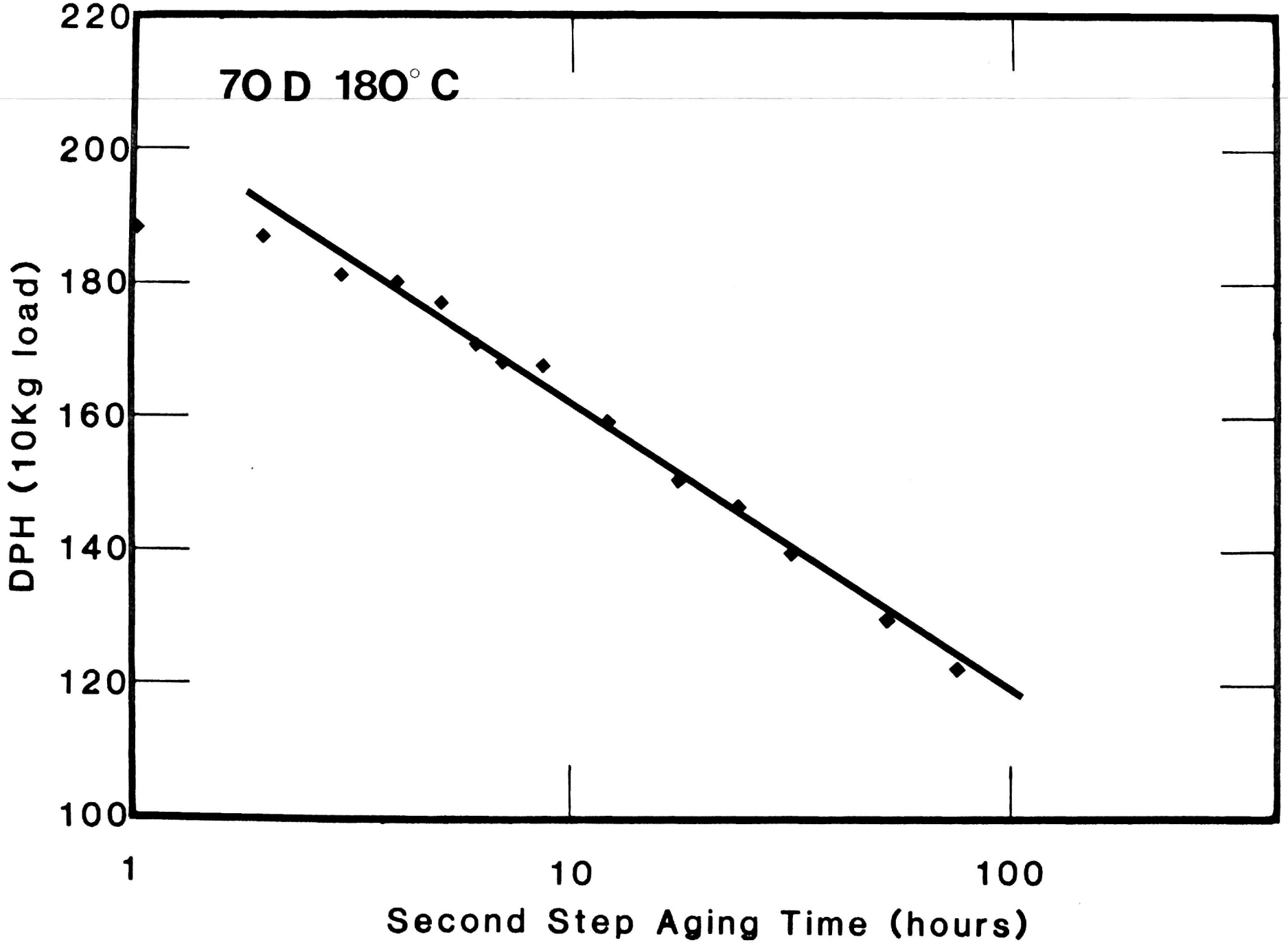

Figure 9. Kinetics of second step aging.

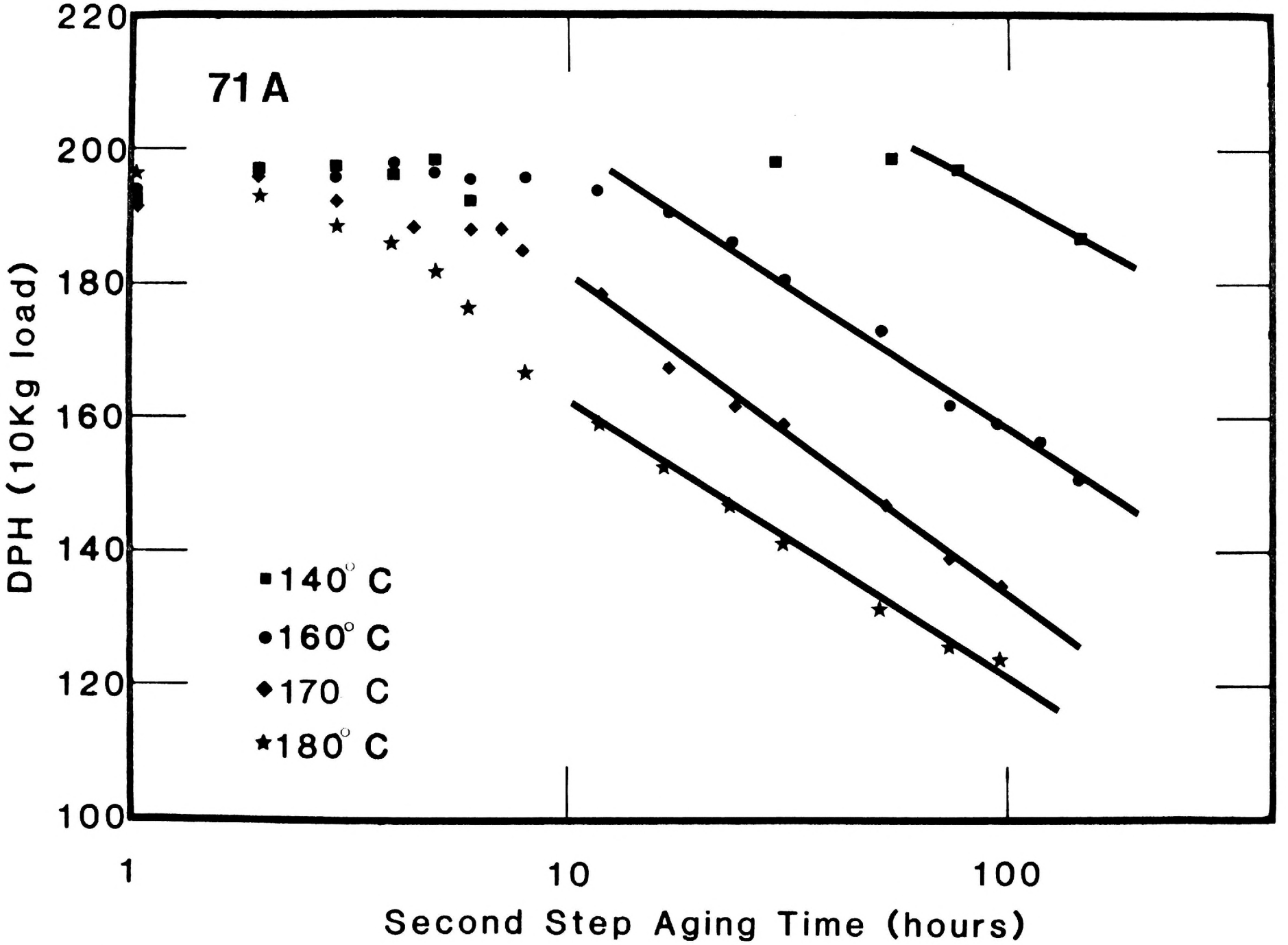

Figure 10. Kinetics of second step aging.

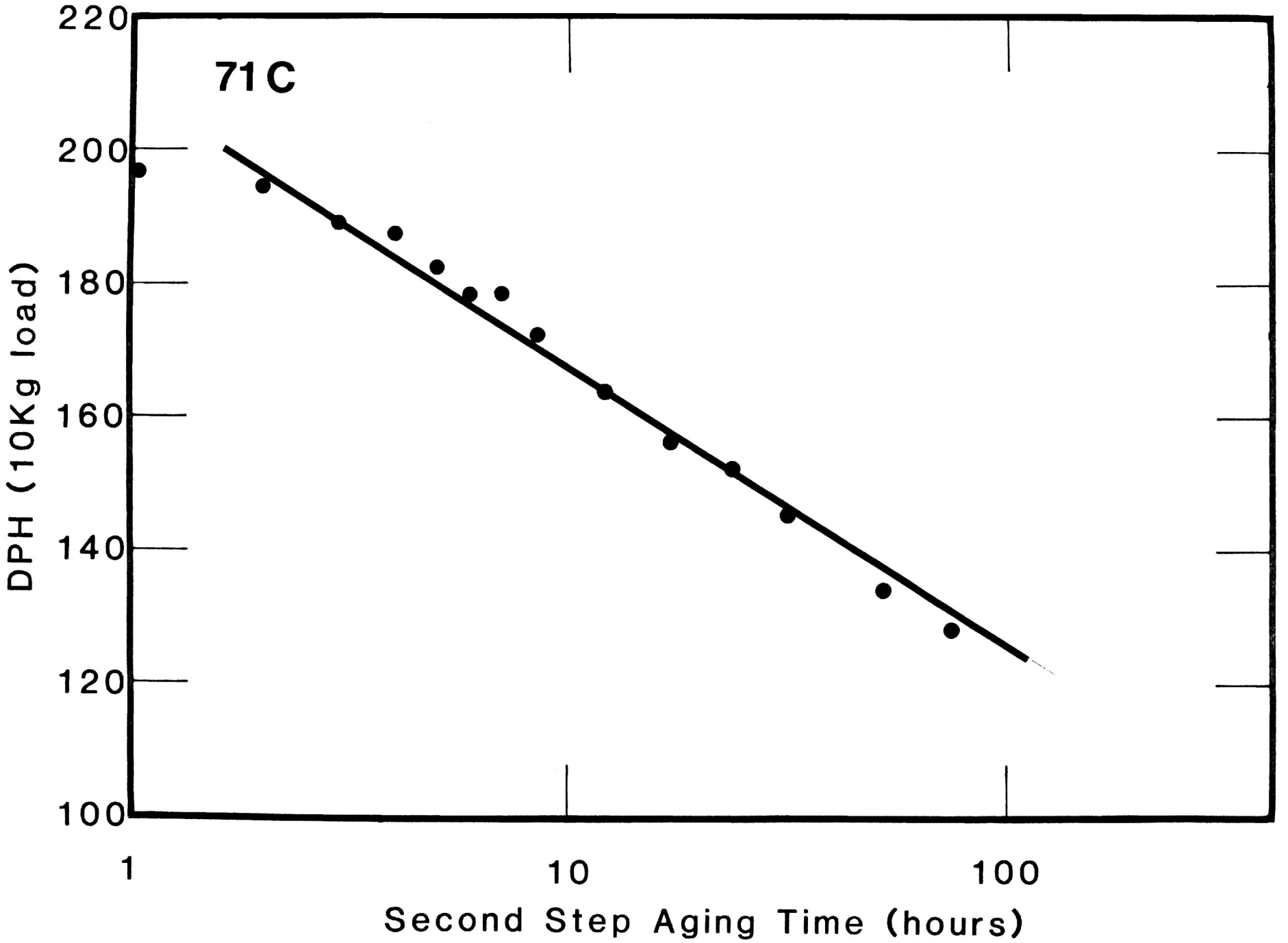

Figure 11. Kinetics of second step aging.

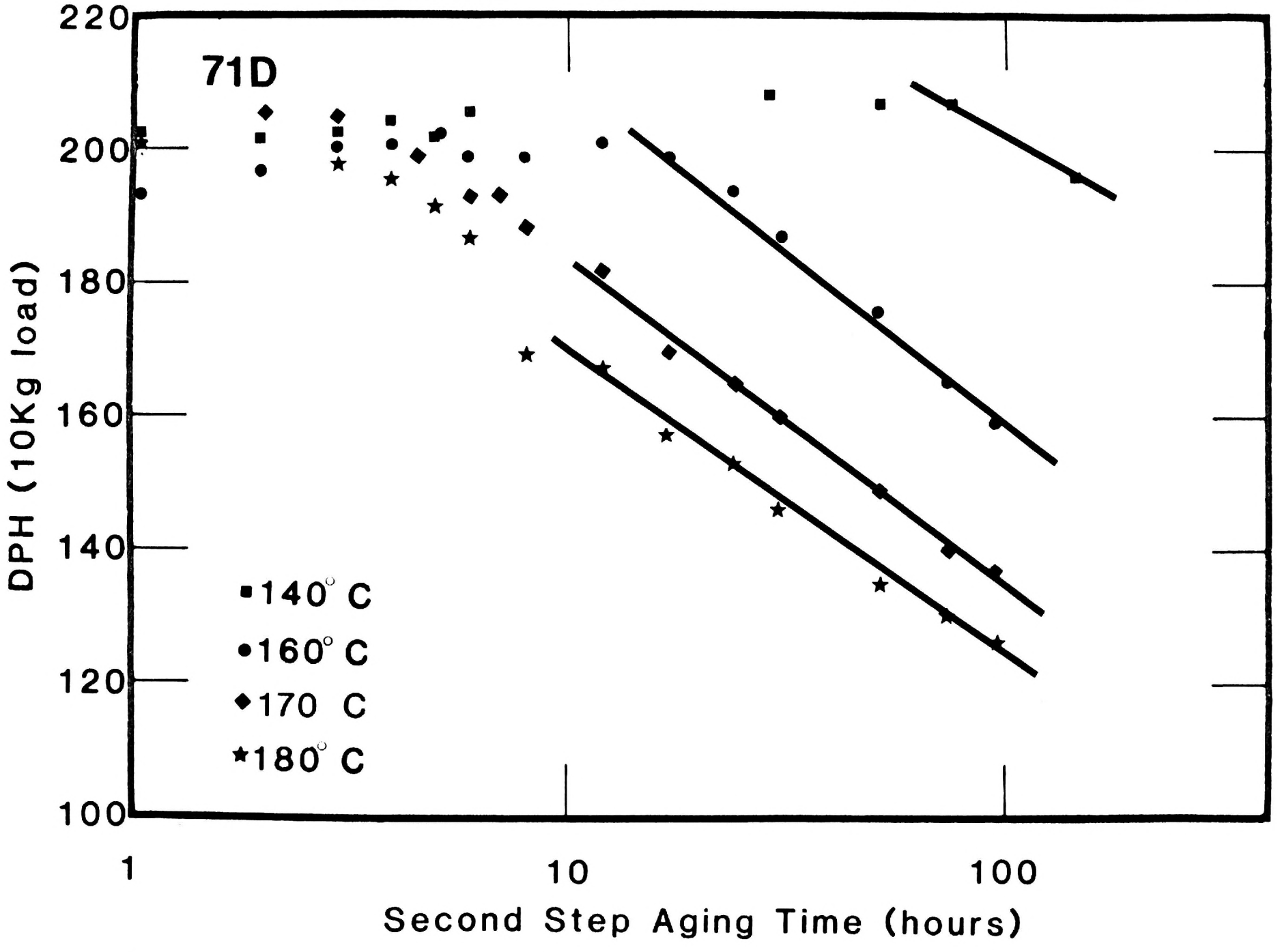

Figure 12. Kinetics of second step aging.